Journal of Cardiovascular Translational Research (2024) 17:669–684
https://doi.org/10.1007/s12265-023-10462-x

REVIEW

A Systematic Approach Focused on Machine Learning Models for Exploring the Landscape of Physiological Measurement and Estimation Using Photoplethysmography (PPG)

Javed Alam[1] · Mohammad Firoz Khan[1] · Meraj Alam Khan[1,2] · Rinky Singh[1] · Mohammed Mundazeer[1] · Pramod Kumar[1]

Received: 17 August 2023 / Accepted: 8 November 2023 / Published online: 27 November 2023

Abstract

A non-invasive optical technique known as photoplethysmography (PPG) can be used to provide various physiological measurements and estimations. PPG can be used to assess cardiovascular disease (CVD). Hypertension is a primary risk factor for CVD and a major health problem worldwide. PPG is popular because of its important applications in the evaluation of cardiac activity, variations in venous blood volume, blood oxygen saturation, blood pressure and heart rate variability, etc. In this study, we provide a comprehensive analysis of the extraction of various physiological parameters using PPG waveforms. In addition, we focused on the role of machine learning (ML) models used for the estimation of blood pressure and hypertension classification based on PPG waveforms to make future research and innovation recommendations. This study will be helpful for researchers, scientists, and medical practitioners working on PPG waveforms for monitoring, screening, and diagnosis, as a comparative study or reference.

Keywords Photoplethysmography · PPG · Estimation · Hypertension · Machine learning · ML · Measurement

Introduction

According to the WHO (World Health Organization), an estimated 17.9 million deaths occur globally each year from cardiovascular disease (CVD), accounting for 31% of all deaths worldwide [1, 2]. The United Nations' Sustainable Development Goals (SDGs) include a target to reduce premature mortality from non-communicable diseases, including cardiovascular diseases, by one-third by 2030. CVD includes cerebrovascular disease, rheumatic heart disease, coronary heart disease, and other conditions that are related to the heart and blood vessels [1]. PPG is a non-invasive optical technique that measures the variation of transmitted and reflected light in terms of intensity [3]. It is a low-cost method, and the resultant signal has several components such as blood vessel wall movement, blood volume, and blood flow in arteries which are associated with cardiac activity [4, 5]. There are so many applications of PPG in healthcare. Many studies have claimed that PPG has the potential for screening, monitoring, and diagnosis of respiratory and cardiovascular disease and neurological disorders, etc. PPG is one of the best options for developing effective and affordable tools for real-time monitoring, screening, and diagnosis [4, 6]. Physiological measurements and estimations play crucial roles in healthcare, research, and personal health management. They help doctors make decisions, track treatment progress, and identify abnormalities or deviations from normal physiological functioning.

A comparative analysis of PPG publications over the past 23 years has been conducted. In this study, the data were obtained from the University of Toronto libraries accessed on 06 June 2023. We searched "photoplethysmography" and found the number of articles with the search criteria, i.e., search for "everything," search scope "All libraries," and language "Any language" with yearly publication. Two different filters were applied to determine the number of published articles. We select the search filters "Any Field" and

Associate Editor Marat Fudim oversaw the review of this article

✉ Javed Alam
javedalam4u@gmail.com

[1] Quantlase Lab LLC, Masdar City, Abu Dhabi, United Arab Emirates

[2] DigiBiomics Inc, Mississauga, Ontario, Canada

"contains" with the search "photoplethysmography" photoplethysmography' with respect to filter 1. As shown in Fig. 1, there has been a significant increase in published papers with respect to the year, and an exponential increase has been observed in the last 10 years. We selected the search filter "Title" and "contains exact phrase" with respect to filter 2. As shown in Fig. 2, there was a significant increase in the number of articles, but the total number of articles was less than that in Fig. 1.

Figure 3 shows a comparative analysis of PPG publications over the past 23 years from the well-known and trusted databases known as PubMed. The PubMed database is maintained by the National Center for Biotechnology Information (NCBI) in the USA. The National Library of Medicine (NLM) is located at the National Institutes of Health (NIH). We searched "photoplethysmography" as the title. Figure 3 clearly shows that there is a significant increase in the number of articles with respect to year. Moreover, Figs. 1, 2 and 3 show a highly positive correlation between the number of published articles on photoplethysmography and the years 2010–2022. Photoplethysmography is popular because of its important applications in the evaluation of cardiac activity, variations in venous blood volume, blood oxygen saturation, blood pressure, heart rate variability, etc.

The regulation of blood pressure in the human body is a complex and multivariate physiological process; therefore, PPG-based blood pressure estimation may not be sufficiently precise [7]. In other words, extracting accurate and precise information from the PPG signal is not easy. Numerous studies have been conducted to extract information from PPG signals. Some authors have used a combination of artificial intelligence (AI) and signal processing algorithms. Artificial intelligence (AI) models can learn complex patterns and waveform variations, enabling more accurate and efficient feature extraction than traditional signal-processing

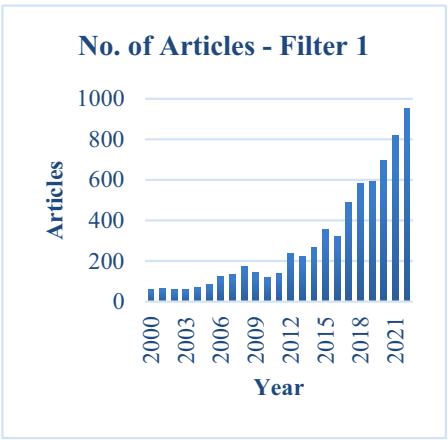

Fig. 1 Published articles trend on Utoronto with filter 1 ("Any Field" and "contains")

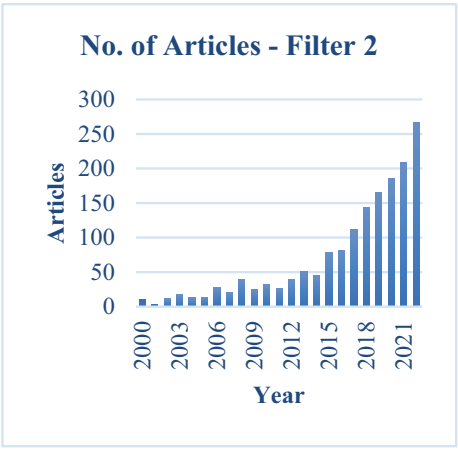

Fig. 2 Published articles trend on Utoronto with filter 2 ("Title" and "contains exact phrase")

methods. ML and deep learning (DL) algorithms are subsets of AI that can be employed to process PPG signals and extract relevant features automatically.

This article's primary contribution revolves around the comprehensive discourse on diverse physiological parameters leveraging PPG and AI/ML coupled with devising healthcare applications through a systematic meticulous review of published scientific literature or recent scholarly works. While the study's objectives are diverse, our specific emphasis is directed towards the following points:

(a) Use of PPG techniques in the field of healthcare.
(b) Presenting an in-depth exposition of distinct physiological measurements and estimations using PPG.
(c) Recent advancements in the utilization of machine learning techniques for blood pressure measurement via PPG are discussed.

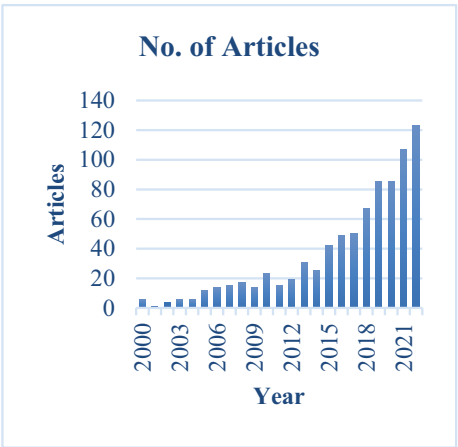

Fig. 3 Published articles trend on PubMed (NCBI data)

(d) Identify and discuss the different machine learning models used for hypertension classification based on PPG.
(e) Outlining prospective and future research directions in the field of PPG.

After elaborating on the introduction and objectives ("Introduction"), the remainder of this article is structured into four additional sections. In "Research methodology," we expound on our research methodology, delving into the details of the data sources, including their identification and search processes, selection criteria, and eligibility parameters. "Results" encompasses the results of the present study. In this section, the different physiological measurements and estimations from PPG, machine learning models used for blood pressure estimation, and hypertension classification based on PPG are discussed comprehensively. Transitioning, in "Discussion," our focus centers on elucidating the limitations and challenges inherent to the study's results. Finally, in "Conclusion and Future Research Recommendations," we provide concluding remarks and recommendations for prospective avenues for future research.

Research Methodology

The Preferred Reporting Items for Systematic Reviews and Meta-analyses (PRISMA) is a well-known, recognized, and accepted guideline for reporting systematic reviews and meta-analyses [2, 4] Therefore, to achieve a valid formulation for systematic reviews, the PRISMA 2020 guidelines were used for this study [8].

Data Source: Identification and Search

So many scientific databases and search engines are available to fulfill the criteria of our research. These include Web of Science, PubMed, Scopus, ProQuest, Elsevier, IEEEXplore, ScienceDirect, and ACM Digital Library. To search the research articles, the keywords "Photoplethysmography" or "PPG" or "Photoplethysmogram" were used to identify all relevant articles. The flowchart of the systematic review according to PRISMA 2020 is shown in Fig. 4. A total number of records were identified from the database and registers were 1474.

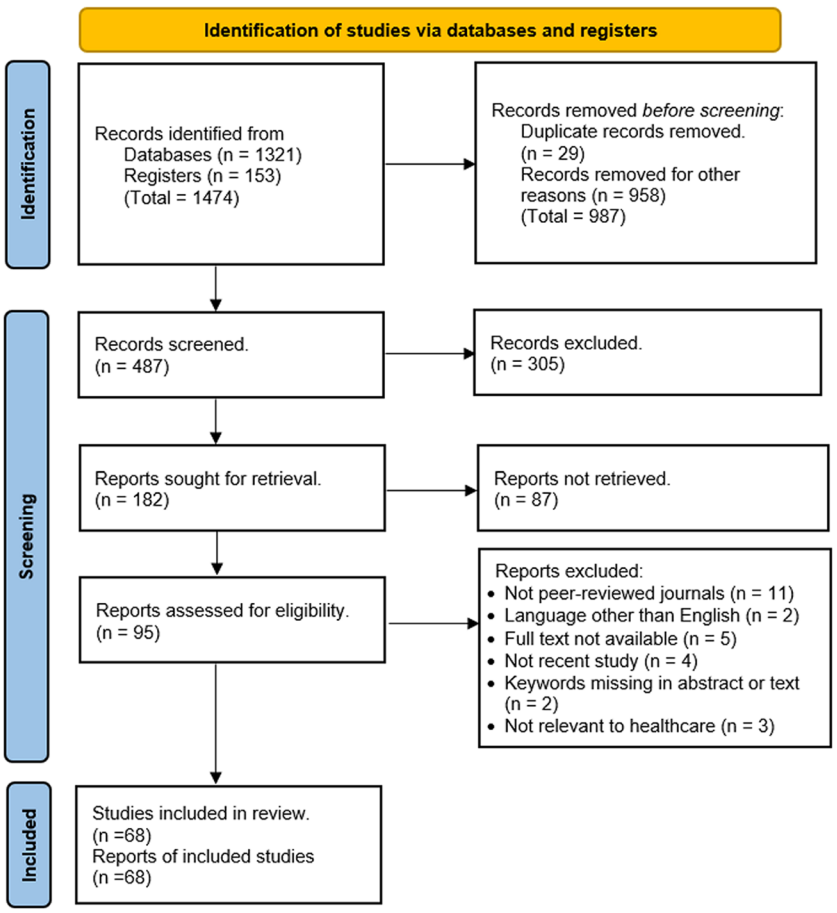

Fig. 4 PRISMA 2020 flowchart illustrating the involved steps undertaken for systematic review

Eligibility Criteria

To ensure the inclusion of relevant studies, the following criteria were used.

(a) The studies were published in peer-reviewed journals or conferences.
(b) The studies were published in English only as a language.
(c) These studies focus more on a recent study, mostly from 2018 to July 2023.
(d) If the study papers were not available in full text, then they should be excluded.
(e) If the keyword was not available in the title or abstract, then it should be excluded.
(f) If the studies were irrelevant to healthcare, they should be excluded.

Selection Process

The abstracts of all included studies were carefully studied and analyzed to determine their relevance in fulfilling our objectives. In this study, we do not use the automation tool for the selection process. The final study selection was performed using the following stepwise criteria:

(a) The studies should be original if any studies were similar or duplicate it was excluded.
(b) Studies that demonstrate the use of photoplethysmography in healthcare have been considered.
(c) The studies only on humans using photoplethysmography were considered.
(d) The studies of the machine learning model used for hypertension classification based on photoplethysmography were considered.
(e) Studies have focused on measuring blood pressure using machine learning from photoplethysmography.

Results

Within the framework of this systematic review, a total of 68 studies were incorporated, after the meticulous screening process that followed the elimination of 987 initial studies. Each of these studies underwent a thorough examination and subsequent classification guided by their thematic alignment with our research objectives. The following subsequent sections present the outcomes of this study.

Physiological Parameters Using Photoplethysmography

Table 1 summarizes the different physiological parameters of the study using PPG. There are many clinical parameters studied using PPG in healthcare. PPG can be utilized in various ways in healthcare such as diagnosis, monitoring, and screening. Different PPG waveforms were used to extract features such as image PPG (iPPG), the first derivative of PPG (FDPPG), velocity waveform of PPG signal (VPG), the second derivative of PPG (SDPPG), and acceleration waveform of PPG signal (APG). The authors recently surveyed the literature on physiological parameters using PPG in healthcare, such as arterial stiffness [9], jugular venous pulse [10], heart rate [11–15], heart rate variability, blood pressure [16–19], blood glucose [20, 21], venous function [22, 23], oxygen saturation [24–27], fetal oxygen saturation [28, 29], respiratory rate [6], lipid profiling [30, 31], cardiac output [32, 33], and ankle brachial pressure [10, 34]. Jugular venous pulse is used to detect right atrial and central venous pressure abnormalities in CVD diagnosis [10].

Blood Pressure Estimation Based on PPG Using Machine Learning Models

There is a comparison of different studies on blood pressure estimation based on PPG using machine learning models. The results are shown in Table 2. The performance of each model and database/number of subjects used in the study based on PPG with SBP and DBP are shown in Table 2. To evaluate the model's performance, different criteria or evaluation metrics have been used. These are mean error (ME), mean absolute error (MAE), mean relative error (MRE), root mean square error (RMSE), standard deviation (STD) or (SD), and ME ± SD. In certain studies, such as those referenced in [37] and [38], the correlation coefficient or Karl–Pearson's coefficient of correlation (r) is employed as an additional performance criterion.

Let E_{i} be the error corresponding to the reference or actual or true blood pressure (BP_{True_i}) and expected or predicted blood pressure (BP_{Pred_i}) in the i th observation or determination, then the error can be defined as follows:

$$E_i = BP_{True_i} - BP_{Pred_i}; i = 1, 2, 3 \ldots \ldots .. n \tag{1}$$

Now, absolute error AE_i and relative error RE_i in the i th observation can be defined as:

$$AE_i = \left| BP_{True_i} - BP_{Pred_i} \right|; i = 1, 2, 3 \ldots \ldots .. n \tag{2}$$

$$RE_i = \frac{\left| BP_{True_i} - BP_{Pred_i} \right|}{BP_{True_i}} = \frac{AE_i}{BP_{True_i}}; i = 1, 2, 3 \ldots \ldots .. n \tag{3}$$

The ME, MAE, MRE, RMSE, and STD are defined as follows:

Table 1 Enlisting a comparative analysis of various physiological parameters studied using photoplethysmography (PPG)

Studies	Published year	Total subject/dataset	Age range (years)	Compared with	Physiological parameter
[9]	2021	12	20–35	N/A	Arterial stiffness and blood pressure
[10]	2020	20 (15 males and 5 females)	23–31	ECG and arterial finger PPG signals for validation	Jugular venous pulse
[11]	2019	5	02–63	Calibrated capnobase dataset of 8-min readings of 42 cases	Heart rate
[16]	2018	N/A	N/A	OMRON BP765CAN Monitor (validated by Hypertension Canada)	Blood pressure
[17]	2018	25 (17 males and 8 females)	18–65	OMRON BP765CAN Monitor (validated by Hypertension Canada)	Blood pressure
[20]	2018	24	20–30	Pathology Laboratory measurements	Blood glucose
[12]	2017	N/A	N/A	Not compared with any reference standard	Heart rate
[13]	2017	To be tested in the future	N/A	Standard heart rate measurement device	Heart rate
[22]	2017	25 (16 females and 9 males)	34–85	Duplex scanning with GE Doppler color flow imaging scanner	Venous function
[14]	2017	10 (6 males and 4 females). Algorithm tested on 35 standard MIMIC data	N/A	BIOPAC MP150	Heart rate
[33]	2016	40 (19 males and 21 females)	15–75	Standard Doppler echo method	Cardiac output
[18]	2016	14 (6 males and 8 females)	22–55	Watch BP Office	Blood pressure
[15]	2015	5	N/A	Medical oximeter	Heart rate, oxygen saturation
[24]	2015	10 (7 males and 3 females)	N/A	Wilcoxon signed-rank test	Oxygen saturation
[28]	2015	1	N/A	Ultrasonic Doppler fetal heart rate detector	Fetal oxygen saturation and fetal heart rate
[30]	2014	76	N/A	Pathology laboratory measurements	Lipid profiling
[6]	2014	4 (females)	N/A	Standard heart rate meter	Respiratory rate
[25]	2014	1	N/A	Clevemed BioRadio	Oxygen saturation
[35]	2013	42 (29 children and 13 adults)	N/A	Capnometry	Respiratory rate
[21]	2012	5	22–35	ARKRAY Glucocard TM 0I-mini	Blood glucose
[36]	2012	Tested on 15819 beats from CSL data set	N/A	Complex System Laboratory (CSL) Benchmark dataset	Respiratory rate
[23]	2011	Several volunteers	N/A	Classical measurement technique probably ultrasound method	Venous function
[19]	2010	23 (6 males and 17 females)	18–60	Sphygmomanometer (Sphy BPM) and automatic BP monitor (Auto BPM)	Blood pressure
[10]	2009	Total 64 limbs = 32 upper limbs and 32 lower limbs	N/A	Auscultatory mercury sphygmomanometer	Ankle brachial pressure
[32]	2009	16 (8 males and 8 females)	22–34	Physio Flow PF-05 impedance cardiograph device	Cardiac output
[29]	2009	6 (healthy pregnant female)	N/A	Biosys IFM 500 Doppler ultrasound fetal monitor system	Fetal oxygen saturation and fetal heart rate
[31]	2007	15	20–59	10-element Windkessel model	Lipid profiling
[26]	2005	1	N/A	Control PPG signal from stationary hand	Oxygen saturation

Table 1 (continued)

Studies	Published year	Total subject/dataset	Age range (years)	Compared with	Physiological parameter
[34]	2005	43	N/A	Continuous wave Doppler method Disadvantage of CW Doppler method: prone to observer error	Ankle brachial pressure
[27]	2005	1	N/A	Nellcor PPG	Oxygen saturation

*N/A not available

$$ME = \frac{1}{N} \times \sum_{i=1}^{n} E_i; i = 1, 2, 3 \ldots \ldots .n \quad (4)$$

$$MAE = \frac{1}{N} \times \sum_{i=1}^{n} |E_i| = \frac{1}{N} \times \sum_{i=1}^{n} AE_i; i = 1, 2, 3 \ldots \ldots .n \quad (5)$$

$$MRE = \frac{1}{N} \times \sum_{i=1}^{n} RE_i; i = 1, 2, 3 \ldots \ldots .n \quad (6)$$

$$RMSE = \sqrt{\frac{1}{N} \times \sum_{i=1}^{n} (E_i)^2}; i = 1, 2, 3 \ldots \ldots .n \quad (7)$$

$$\text{STD or SD} = \sqrt{\frac{1}{N} \times \sum_{i=1}^{n} (E_i - ME)^2}; i = 1, 2, 3 \ldots \ldots .n \quad (8)$$

where N is the total number of observations (test segments or samples). The above performance criteria were used to measure systolic blood pressure (SBP) as well as diastolic blood pressure (DBP).

Several types of machine learning models can be used for blood pressure estimation using photoplethysmography signals. Linear regression [64], polynomial regression, or a support vector machine (SVM) [60, 61, 63] can be used to establish a relationship between the extracted features from PPG signals and blood pressure values. These models learn a mapping function between the input features and the target output (blood pressure) and can provide continuous blood pressure estimates. Feedforward Neural Networks [40], multilayer perceptron (MLP), autoencoder [45, 47], modified U-net, Cycle Generative Adversarial Network [43], Residual Network (ResNet), and Gaussian Process Regression (GPR) [38] can be used for blood pressure estimation. Convolutional Neural Networks (CNN) [41] and Artificial Neural Networks (ANN) [46] are effective for learning spatial features from PPG signals. They are particularly useful for analyzing the temporal patterns and morphological characteristics of PPG waveforms. Recurrent Neural Networks (RNN) [46], Long Short-Term Memory (LSTM) [42, 45], Bidirectional LSTM (Bi-LSTM) [48, 49], and gated recurrent units (GRU) [48] are suitable for modeling temporal dependencies in PPG signals. Ensemble models such as Gradient Boosting, CatBoost [38], and Adaptive Boosting (AdaBoost) [53, 54, 59] leverage the diversity of different models to obtain more accurate blood pressure estimates using PPG signals. Deep Neural Networks (DNN) [51] can be utilized to build complex models with multiple layers for blood pressure estimation.

Each ML model was applied to one of the well-known databases such as MIMIC, MIMIC II [66], MIMIC III [67], PPG-BP [68], VitalDB, and Queensland for measuring BP. As shown in Table 2, in studies [40, 44, 49, 52], they were used different databases with a smaller number of subjects. In a recent study by [39], they applied SVR, CatBoost, LightGBM, and XGBoost machine learning models to predict BP. In this study, they used PPG waveform from the MIMIC III database and extracted 38 features from three categories namely semi-classical signal analysis (SCSA), SDPPG, and PPG. The authors showed that the CatBoost algorithm was better than the SVR, LightGBM, and XGBoost algorithms. The CatBoost algorithm achieved a mean absolute error of 5.37 mmHg with a standard deviation of 5.56 mmHg and 2.96 mmHg with a standard deviation of 3.13 mmHg for systolic and diastolic blood pressure, respectively. A previous study [41] estimated a mean absolute error of 5.73 mmHg and 3.45 mmHg for SBP and DBP respectively by using the CNN learning model. Previous studies [42, 49, 52, 56] use an electrocardiogram (ECG) and PPG waveforms to measure SBP and DBP.

Machine Learning Model Used for Hypertension Classification

Hypertension (HT), also known as high blood pressure (high BP), stands as the primary risk factor for CVD. In 2015, a report by the World Health Organization (WHO) indicated that 1.13 billion people were suffering from hypertension (HT) [69]. The 7th report of the US Joint National Committee on Prevention, Detection, Evaluation, and Treatment of High Blood Pressure (JNC7) categorized the blood pressure level

Table 2 Comparison of blood pressure estimation models used in different studies

Studies	Published year	ML model	Database/number of subjects	Performance criteria	SBP (mmHg)	DBP (mmHg)
[39]	2023	CatBoost	MIMIC III (38 features of SCSA, SDPPG, PPG)	Mean absolute error Standard deviation of AE	**5.37** **5.56**	**2.96** **3.13**
[40]	2023	Feedforward Deep NN with ANN Model	25 subjects	Mean absolute error Mean error Standard deviation of error	**7.41** **−4.02** **10.40**	**3.32** **−0.31** **4.89**
[41]	2022	CNN (U-Net)	MIMIC III (942 subjects)	Mean absolute error	**5.73**	**3.45**
[42]	2022	ResNet + LSTM	MIMIC (PPG + ECG)	Mean absolute error Root mean squared error	**4.18** **5.68**	**2.28** **2.99**
[43]	2022	Cycle Generative Adversarial Network	MIMIC II (90 subjects, PPG, ABP signal)	Mean absolute error Root mean squared error	**2.29** **3.22**	**1.93** **2.61**
[44]	2022	ANN	30 subjects	Mean absolute error Mean error Standard deviation of error	**8.89** **2.52** **12.15**	**4.92** **0.59** **7.07**
[45]	2021	LSTM-Autoencoder	MIMIC II, 5289 subjects, PPG	Mean absolute error Root mean squared error	**4.05** **5.25**	**2.41** **3.17**
[46]	2021	ANN + RNN	VitalDB (1376 subjects, 28 PPG features)	Mean absolute difference Standard deviation of errors Root mean squared error	**5.07** **6.92** **6.92**	**2.86** **3.99** **3.99**
[47]	2021	Autoencoder	MIMIC II (PPG, ABP raw signals)	Mean absolute error	**5.42**	**3.14**
[48]	2021	Bi-LSTM	PPG-BP	Mean absolute error Root mean squared error	**4.93 ± 4.40** **7.38**	**4.18 ± 4.43** **8.23**
[48]	2021	GRU	PPG-BP	Mean absolute error Root mean squared error	**3.68 ± 4.28** **6.11**	**5.34 ± 5.24** **8.22**
[49]	2021	Bi-LSTM	Anonymous (18 patiens; ECG, PPG, BCG features)	Mean absolute error Root mean squared error	**5.82** **6.82**	**5.24** **6.06**
[37]	2021	Modified U-net	MIMIC I, MIMIC III (PPG raw)	Mean absolute error Standard deviation Root mean squared error Pearson's correlation Coefficient	**3.68** **4.42** **5.75** **0.98**	**1.97** **2.92** **3.52** **0.97**
[50]	2021	Bi-GRU + GRU + attention	MIMIC II (PPG-500 segments, 59 PPG features)	MAE SD	**2.58** **± 3.35**	**1.26** **± 1.63**
[51]	2020	DNN	MIMIC II (PPG features, 9000 subjects)	Mean absolute error Root mean squared error	**3.21** **4.63**	**2.23** **3.21**
[38]	2020	Gaussian Process Regression (GPR)	222 recordings, 126	Mean absolute error Mean squared error Root mean squared error Coefficient of correlation	**3.02** **45.49** **6.74** **0.95**	**1.74** **12.89** **3.59** **0.96**
[52]	2020	CNN + Bi-GRU + Attention	15 subjects (ECG, PPG, BCG features)	Mean absolute error Root mean squared error SD	**4.06** **5.42** **4.04**	**3.33** **4.30** **3.42**
[53]	2020	AdaBoost	MIMIC II (19 PPG features)	Mean absolute error Standard deviation of AE Coefficient of correlation	**8.22** **10.38** **0.78**	**4.17** **4.22** **0.72**
[54]	2019	AdaBoost	MIMIC II (1323 PPG signal, PPG, SDPPG features)	Mean absolute error Root mean squared error Standard deviation of errors Standard deviation of AE	**3.97** **8.9** **8.90** **7.99**	**2.43** **4.18** **4.17** **3.37**
[55]	2019	Deep learning (spectro-temporal ResNet)	MIMIC III, 510 subjects	Mean absolute error	**9.43**	**6.88**

Table 2 (continued)

Studies	Published year	ML model	Database/number of subjects	Performance criteria	SBP (mmHg)	DBP (mmHg)
[56]	2018	DNN	85 subjects (ECG, PPG features)	Mean absolute difference Root mean squared error	**3.31** **4.60**	**2.22** **3.15**
[57]	2018	Deep learning (long short-term memory (LSTM)	84 subjects	Root mean squared error	**3.73**	**2.43**
[58]	2018	Autoregressive moving average (ARMA) models	15 subjects	Root mean squared error	**6.49**	**4.33**
[59]	2017	AdaBoost	MIMIC, 942 subjects, PAT, HR time interval	Mean absolute error Standard deviation Coefficient of correlation	**11.57** **10.09** **0.59**	**5.35** **6.14** **0.48**
[60]	2017	Neural Network	MIMIC II, 910 subjects	Mean absolute error Root mean square deviation	**13.4** **11.6**	**6.9** **5.9**
[60]	2017	SVM	MIMIC II, 910 subjects	Mean absolute error Root mean square deviation	**8.54** **10.9**	**4.34** **5.8**
[61]	2017	SVM	Queensland (7000 samples from 32 patients)	Mean absolute error	**11.64**	**7.62**
[61]	2017	Neural Network (9 input neurons)	Queensland (7000 samples from 32 patients)	Mean absolute error	**11.89**	**8.83**
[62]	2016	FFT-based ANN	MIMIC II	Beat-to-beat fitting error	$\mathbf{0.06 \pm 7.08}$	$\mathbf{0.01 \pm 4.66}$
[63]	2015	SVM	MIMIC II (1000)	Mean absolute error	**12.38**	**6.34**
[64]	2013	Linear Regression	MIMIC, more than 15,000 samples	Mean absolute error Mean relative error	$\mathbf{9.80 \pm 8.09}$ $\mathbf{8.94 \pm 7.57}$	$\mathbf{5.88 \pm 5.11}$ $\mathbf{10.26 \pm 8.83}$
[64]	2013	Neural Network (4 input neurons)	MIMIC, more than 15,000 samples	Mean absolute error Mean relative error	$\mathbf{5.19 \pm 5.01}$ $\mathbf{4.73 \pm 4.59}$	$\mathbf{2.91 \pm 2.92}$ $\mathbf{5.02 \pm 4.80}$
[64]	2013	Neural Network (12 input neurons)	MIMIC, more than 15,000 samples	Mean absolute error Mean relative error	$\mathbf{3.80 \pm 3.46}$ $\mathbf{3.48 \pm 3.19}$	$\mathbf{2.21 \pm 2.09}$ $\mathbf{3.90 \pm 3.51}$
[65]	2009	Proprietary Algorithm	MIMIC, 34 recordings, 25	Mean squared error	**70.05**	**35.08**

of adults into normotension (NT), prehypertension (PHT), and hypertension (HT) [70]. Many studies have been conducted into three classes namely NT vs. PHT, NT vs. HT, and (NT + PHT) vs. HT. Many assessment criteria are available in the literature such as specificity, sensitivity, accuracy, F1-score, precision, area under the curve (AUC) and receiver operating characteristic curve (ROC), Matthew's correlation coefficient, and Cohen's kappa coefficient. Mostly, the authors used the F1-score as a performance criterion of the ML models. In Table 3, we show the F1-score as a performance criterion of the model achieved by the ML classifier for hypertension classification. The F1-score was calculated using the following formula [71]:

$$F_1 Score = 2 \times \frac{Precision \times Recall}{Precision + Recall} = \frac{TP}{TP + \frac{1}{2}(FP + FN)} \tag{9}$$

where

$$Precision = \frac{TP}{TP + FP} \tag{10}$$

$$Recall = \frac{TP}{TP + FN} \tag{11}$$

where TP = true positive, FP = false positive, FN = false negative.

In Table 3, detailed descriptions related to the hypertension classification model are shown such as database, required signal, and features used by the researchers. A variety of ML classifiers were proposed for hypertension classification. Some of the widely used algorithm/ML classifiers are k-Nearest Neighbors (KNN) [7, 75], Naïve Bayes [74], Logistic Regression [75], Random Forest [74], SVM [72], AdaBoost [75], and Bagged Tree [75]; these are ease of modelling for a complex problem. In our finding, some authors proposed modern neural network architectures such as LightGBM [70], AlexNet [73], DenseNet [73], GoogleNet [73, 76], and ResNet [73]. In the study [69], they used a hybrid classifier known as Adaptive Neuro-fuzzy Inference System (ANFIS), a combination of ANN and fuzzy-set theory and widely used in medical diagnostic systems.

Table 3 Analytical comparison of hypertension classification models used in various studies

Studies	Published year	Database	Signal required	Features used	Class	Training and testing tatio (%)	ML classifier	F1-score (%)
[69]	2023	DataCite (657 data records 219 patients)	PPG	20 top features using correlation with SBP and DBP	NT(237) vs. PHT(258) NT(237) vs. HT1(102) NT(237) vs. HT2(60)	80:20	ANFIS	92.00 98.5 98.3
[70]	2023	MIMIC III (121 subjects, 2958 segments for classification)	PPG	PPG-189 features	NT (1158) vs. PHT (950) NT (1158) vs. HT (850) NT + PHT (2108) vs HT (850)	70:30	LightGBM	86.57 94.18 91.70
[70]	2023	MIMIC III (121 subjects)	PPG	VPG-200 features	NT (1158) vs. PHT (950) NT (1158) vs. HT (850) NT + PHT (2108) vs HT (850)	70:30	LightGBM	89.41 94.85 91.93
[70]	2023	MIMIC III (121 subjects)	PPG	APG-190 features	NT (1158) vs. PHT (950) NT (1158) vs. HT (850) NT + PHT (2108) vs HT (850)	70:30	LightGBM	86.21 94.86 89.45
[70]	2023	MIMIC III (121 subjects)	PPG	PPG-189 features, VPG-200 features	NT (1158) vs. PHT (950) NT (1158) vs. HT (850) NT + PHT (2108) vs HT (850)	70:30	LightGBM	89.58 95.84 92.5
[70]	2023	MIMIC III (121 Subjects)	PPG	PPG -189 features, APG-190 features	NT (1158) vs. PHT (950) NT (1158) vs. HT (850) NT + PHT (2108) vs HT (850)	70:30	LightGBM	88.62 97.01 92.18
[70]	2023	MIMIC III (121 subjects)	PPG	VPG-200 features, APG-190 features	NT (1158) vs. PHT (950) NT (1158) vs. HT (850) NT + PHT (2108) vs HT (850)	70:30	LightGBM	89.08 96.51 92.06
[70]	2023	MIMIC III (121 subjects)	PPG	PPG -189 features VPG-200 features APG-190 features	NT (1158) vs. PHT (950) NT (1158) vs. HT (850) NT + PHT (2108) vs HT (850)	70:30	LightGBM	90.18 97.51 92.77
[72]	2022	Clinical data-PPG-BP (219 subjects)	PPG	19 WST features	NT (37%) vs. PHT (38%)	75:25	SVM	76.00

Table 3 (continued)

Studies	Published year	Database	Signal required	Features used	Class	Training and testing tatio (%)	ML classifier	F1-score (%)
[72]	2022	Clinical data-PPG-BP (219 subjects)	PPG	Age, BMI, heart rate	NT (37%) vs. PHT (38%)	75:25	SVM	69.57
[72]	2022	Clinical data-PPG-BP (219 subjects)	PPG	Age, BMI, heart rate, plus 19 WST features	NT (37%) vs. PHT (38%)	75:25	Early fusion KNN	69.77
[72]	2022	Clinical data-PPG-BP (219 subjects)	PPG	Age, BMI, heart rate, plus 19 WST features	NT (37%) vs. PHT (38%)	75:25	Late fusion (SVM + SVM + LR)	72.34
[73]	2021	MIMIC (582 data for 10 s each)	PPG	PPG, VPG, APG	NT vs. PHT NT vs. HT NT + PHT vs. HT	70:30	AlexNet (8—layers)	85.80 98.90 93.54
[73]	2021	MIMIC (582 data for 10 s each)	PPG	PPG, VPG, APG	NT vs. PHT NT vs. HT NT + PHT vs. HT	70:30	ResNet18 (18—layers)	84.37 94.09 88.52
[73]	2021	MIMIC (582 data for 10 s each)	PPG	PPG, VPG, APG	NT vs. PHT NT vs. HT NT + PHT vs. HT	70:30	GoogLeNet (22—layers)	80.03 89.24 83.46
[73]	2021	MIMIC (582 data for 10 s each)	PPG	PPG, VPG, APG	NT vs. PHT NT vs. HT NT + PHT vs. HT	70:30	ResNet (34—layers)	84.77 94.01 88.39
[7]	2020	PPG-BP figshare (121 subjects)	PPG	PPG features	NT (46) vs. PHT (41) NT (46) vs. HT (34) NT + PHT (87) vs HT (34)	N/A	KNN	100 100 90.90
[74]	2020	MIMIC II (526906 items)	PPG	PPG features	NT (353840) vs. PHT (116879) NT (353840) vs. HT (56187) NT + PHT (470,719) vs HT (56187)	Vary from class to class	Random Forest	85.70 98.30 93.30
[74]	2020	MIMIC II (526906 items)	PPG	PPG features	NT (353840) vs. PHT (116879) NT (353840) vs. HT (56187) NT + PHT (470719) vs HT (56187)	Vary from class to class	Naive Bayes	82.80 99.40 91.60

Table 3 (continued)

Studies	Published year	Database	Signal required	Features used	Class	Training and testing tatio (%)	ML classifier	F1-score (%)
[75]	2018	MIMIC (121 subjects)	PPG and ECG	PAT and 10 PPG features	NT (46) vs. PHT (41) NT (46) vs. HT (34) NT + PHT (87) vs HT (34)	70:30	AdaBoost Tree	74.67 90.15 79.71
[75]	2018	MIMIC (121 subjects)	PPG	10 PPG features	NT (46) vs. PHT (41) NT (46) vs. HT (34) NT + PHT (87) vs HT (34)	70:30	AdaBoost Tree	72.76 80.11 63.79
[75]	2018	MIMIC (121 Subjects)	PPG and ECG	PAT features	NT (46) vs. PHT (41) NT (46) vs. HT (34) NT + PHT (87) vs HT (34)	70:30	AdaBoost Tree	66.88 68.10 53.19
[75]	2018	MIMIC (121 subjects)	PPG and ECG	PAT and 10 PPG features	NT (46) vs. PHT (41) NT (46) vs. HT (34) NT + PHT (87) vs HT (34)	70:30	Bagged Tree	83.88 94.13 88.22
[75]	2018	MIMIC (121 subjects)	PPG	10 PPG features	NT (46) vs. PHT (41) NT (46) vs. HT (34) NT + PHT (87) vs HT (34)	70:30	Bagged Tree	78.48 84.98 75.32
[75]	2018	MIMIC (121 subjects)	PPG and ECG	PAT features	NT (46) vs. PHT (41) NT (46) vs. HT (34) NT + PHT (87) vs HT (34)	70:30	Bagged Tree	66.95 68.10 53.19
[75]	2018	MIMIC (121 subjects)	PPG and ECG	PAT and 10 PPG features	NT (46) vs. PHT (41) NT (46) vs. HT (34) NT + PHT (87) vs HT (34)	70:30	Logistic Regression	63.92 79.11 62.26
[75]	2018	MIMIC (121 subjects)	PPG	10 PPG features	NT (46) vs. PHT (41) NT (46) vs. HT (34) NT + PHT (87) vs HT (34)	70:30	Logistic Regression	63.66 67.94 47.10

Table 3 (continued)

Studies	Published year	Database	Signal required	Features used	Class	Training and testing tatio (%)	ML classifier	F1-score (%)
[75]	2018	MIMIC (121 subjects)	PPG and ECG	PAT features	NT (46) vs. PHT (41) NT (46) vs. HT (34) NT + PHT (87) vs HT (34)	70:30	Logistic Regression	56.85 67.85 52.38
[75]	2018	MIMIC (121 subjects)	PPG and ECG	PAT and 10 PPG features	NT (46) vs. PHT (41) NT (46) vs. HT (34) NT + PHT (87) vs HT (34)	70:30	KNN	84.34 94.84 88.49
[75]	2018	MIMIC (121 subjects)	PPG	10 PPG features	NT (46) vs. PHT (41) NT (46) vs. HT (34) NT + PHT (87) vs HT (34)	70:30	KNN	78.62 86.94 78.44
[75]	2018	MIMIC (121 subjects)	PPG and ECG	PAT features	NT (46) vs. PHT (41) NT (46) vs. HT (34) NT + PHT (87) vs HT (34)	70:30	KNN	53.93 54.08 53.01
[76]	2018	MIMIC (121 subjects)	PPG	CWT scalogram	NT (46) vs. PHT (41) NT (46) vs. HT (34) NT + PHT (87) vs HT (34)	80:20	GoogLeNet	80.52 92.55 82.95

Discussion

The British Hypertension Society (BHS) and the Association for Advancement of Medical Instrumentation (AAMI) are two types of performance indicators used as BP monitoring global standard [52]. As shown in Table 4, the BHS standard provides the Grades namely A, B, C, and D according to the different ranges of MAE with the proportion of subjects. According to BHS standard, the model achieved at least grade B for SBP and DBP predictions [47].

As shown in Table 5, the AAMI standard sets establish the range for the mean absolute error (MAE), standard deviation (SD), and size of the population (subjects or sample).

The performance criteria of the SBP and DBP estimation models were evaluated using MAE ± SD. As mentioned in Table 5, MAE and SD should be less than 5 mmHg and 8 mmHg respectively according to AAMI standard. As shown in Table 2, many ML models do not fulfill the AAMI

Table 4 Grade and MAE value with BHS Standard

BHS grade	Proportion of the subjects with MAE		
	MAE ≤ 5 mmHg	MAE ≤ 10 mmHg	MAE ≤ 15 mmHg
A	60%	85%	95%
B	50%	75%	90%
C	40%	65%	85%
D	Worse than C		

Table 5 AAMI International Standard Range

Mean absolute error	Standard deviation	Subjects
≤ 5	≤ 8	≥ 85

standard for evaluating SBP such as [39, 40, 53, 60, 61, 63]. Moreover, as shown in Table 1, many studies were performed with less than 15 subjects which was insufficient because the AAMI standards require at least 85 subjects.

A recent study done by [70] achieved a higher F1-score with LightGBM ML classifier for hypertension when they used 189 features from PPG, 200 features from VPG, and 190 features from APG. In their study [73], they applied deep learning architectures namely AlexNet, ResNet, and GoogLeNet based on the Hilbert–Huang Transform (HHT) method to predict the hypertension level and achieved higher F1-scores using AlexNet than ResNet and GoogLeNet. They applied the model on the MIMIC dataset and PPG, VPG, and APG features were used. In another study [7] were proposed a KNN model to classify the BP applied on PPG–BP figshare data. The PPG–BP figshare database [68] was collected from 219 subjects while they used 121 subjects which were divided into normotensive (46 subjects), pre-hypertensive (41 subjects), and hypertensive (34 subjects). The F1-scores with three classification trials as NT vs. PHT, NT vs. HT, and NT + PHT vs. HT. were 100%, 100%, and 90.90%, respectively. They showed that the KNN model is superior to the model proposed by [75] (KNN, AdaBoost, Bagged Tree, Logistic Regression) whereas Liang et al. 2018a used the MIMIC database, PPG, and PAT features. The disadvantage of extracting PPG features is the requirement for the finest PPG waveform [72]. Moreover, calculating PAT features from PPG and ECG signals is complicated because it requires stable and high-quality synchronized waveforms.

Conclusion and Future Research Recommendations

This study offers a systematic review of physiological measurements and estimations obtained using photoplethysmography (PPG). This has significant clinical relevance in various healthcare domains such as diagnosis, monitoring, and screening. It includes the capabilities and constraints of PPG usage through a systematic analysis of diverse research in healthcare and the advancement of machine learning methods for estimation and classification. Thus, this study empowers researchers and clinicians with the knowledge required to make informed decisions regarding PPG utilization. The outcomes of this thorough investigation revealed that PPG holds potential for healthcare diagnosis, monitoring, and screening, particularly when combined with machine learning (ML) or deep learning (DL) algorithms to enhance computational capacity and achieve heightened accuracy. However, certain gaps in the existing literature are still evident and that will be undertaken by future studies. According to our findings, many studies have compared the accuracy of the ML model without any consideration of the database and features used in the model. To achieve higher accuracy with the ML/DL model, the data should be more aligned, accurate, and precise, which is a significant challenge for PPG. Advanced deep learning frameworks, such as LightGBM, AlexNet, DenseNet, GoogleNet, and ResNet, have the potential to yield superior accuracy. However, they require extensive training time, heightened processing capabilities, and increased resources. Consequently, these frameworks can substantially amplify the computational intricacies of the system [39].

Based on the literature exploration, proposing recommendations that can be considered to solve clinical problems by using PPG as follows: (i) early precise detection and prediction—investigate the potential of PPG-derived features and machine learning algorithms for early detection and prediction of cardiovascular diseases, such as heart failure, hypertension, and arrhythmias; (ii) multi-modal analysis—explore the integration of PPG with other physiological signals, such as electrocardiography (ECG) and accelerometer data, to develop a comprehensive and accurate cardiovascular health monitoring system; (iii) novel biomarkers—identify novel PPG-based biomarkers that can provide insights into cardiovascular health, such as arterial stiffness, pulse wave velocity, and cardiac output, and correlate these biomarkers with disease progression; (iv) personalized risk assessment—develop a personalized risk assessment model that utilizes PPG data along with patient-specific information (age, sex, medical history) to estimate an individual's risk of developing cardiovascular diseases; (v) ambulatory monitoring—design wearable PPG devices for continuous ambulatory monitoring, allowing for real-time tracking of cardiovascular parameters during daily activities and sleep, which could aid in understanding disease patterns; (vi) stress and emotional analysis—explore the relationship between PPG signals and stress levels or emotional states, as chronic stress is a risk factor for cardiovascular diseases. Develop algorithms to detect stress-induced changes in PPG patterns and (vii) large-scale data analysis—conduct large-scale data analysis using PPG data from diverse populations to uncover potential disparities and variations in cardiovascular health and disease outcomes.

While PPG is a valuable and convenient tool for physiological measurement and estimation, it may not be as accurate or reliable as more direct and invasive measurement methods in certain clinical scenarios. There are various factors such as motion artifacts, ambient light interference, skin pigmentation, and device calibration that can affect the accuracy of PPG measurements. Therefore, proper calibration and consideration of these factors are essential for obtaining meaningful and reliable physiological data from PPG. The monitoring of mental health based on PPG technology is an exciting field, but more collaboration is needed between

software engineers, sensor manufacturers, and medical practitioners to provide a jumpstart [4].

Acknowledgements We are deeply grateful for the financial support provided by Quantlase Lab LLC Abu Dhabi, UAE. We would also like to express our gratitude to the management of Quantlase Lab for their visionary leadership and encouragement. We feel deeply indebted to Mr. Sheraz Raza Siddiqui, Executive Director, Quantlase Lab LLC Abu Dhabi for his guidance, advice, and encouragement throughout the period of this research. We would like to extend our sincere gratitude to Dr. Azam Ali Khan and Dr. Nuzhat Ahsan, Quantlase Lab, for the fruitful discussions during the preparation of this manuscript. We extend our sincere appreciation to the entire team at Quantlase Lab for their collaborative spirit and dedication.

Declarations

Conflict of Interest The authors declare no competing interests.

References

1. García-López I, Rodriguez-Villegas E. Extracting the jugular venous pulse from anterior neck contact photoplethysmography. Sci Rep. 2020;10. https://doi.org/10.1038/s41598-020-60317-7.
2. Lazim MRMLM, Aminuddin A, Chellappan K, Ugusman A, Hamid AA, Ahmad WANW, Mohamad MSF. Is heart rate a confounding factor for photoplethysmography markers? A systematic review, Int J Environ Res Public Health. 2020;17. https://doi.org/10.3390/ijerph17072591.
3. Zaunseder S, Trumpp A, Wedekind D, Malberg H. Cardiovascular assessment by imaging photoplethysmography-a review. Biomedizinische Technik. 2018;63. https://doi.org/10.1515/bmt-2017-0119.
4. Almarshad MA, Islam MS, Al-Ahmadi S, BaHammam AS. Diagnostic features and potential applications of PPG signal in healthcare: a systematic review. Healthcare. 2022;10:547. https://doi.org/10.3390/healthcare10030547.
5. Biswas D, Simoes-Capela N, Van Hoof C, Van Helleputte N. Heart rate estimation from wrist-worn photoplethysmography: a review. IEEE Sens J. 2019;19. https://doi.org/10.1109/JSEN.2019.2914166.
6. Daimiwal N, Sundhararajan M, Shriram R. Respiratory rate, heart rate and continuous measurement of BP using PPG, in: International Conference on Communication and Signal Processing. ICCSP 2014 – Proceedings. 2014. https://doi.org/10.1109/ICCSP.2014.6949996.
7. Tjahjadi H, Ramli K. Noninvasive blood pressure classification based on photoplethysmography using K-nearest neighbors' algorithm: a feasibility study. Information (Switzerland). 2020;11. https://doi.org/10.3390/info11020093.
8. Namvari M, Lipoth J, Knight S, Jamali AA, Hedayati M, Spiteri RJ, Syed-Abdul S. Photoplethysmography enabled wearable devices and stress detection: a scoping review. J Pers Med. 2022;12. https://doi.org/10.3390/jpm12111792.
9. Djeldjli D, Bousefsaf F, Maaoui C, Bereksi-Reguig F, Pruski A. Remote estimation of pulse wave features related to arterial stiffness and blood pressure using a camera. Biomed Signal Process Control. 2021;64. https://doi.org/10.1016/j.bspc.2020.102242.
10. Sun X, Liu C, Zhang Y, Yang L. An automatic instrument for brachial and ankle systolic pressure measurement using photoplethysmography. In: 3rd International Conference on Bioinformatics and Biomedical Engineering, ICBBE 2009. 2009. https://doi.org/10.1109/ICBBE.2009.5162312.
11. Y. Aarthi, B. Karthikeyan, N.P. Raj, M. Ganesan, Fingertip based estimation of heart rate using photoplethysmography, in: 2019 5th International Conference on Advanced Computing and Communication Systems, ICACCS 2019, 2019. https://doi.org/10.1109/ICACCS.2019.8728432.
12. Meddah K, Kedir-Talha M, Zairi H. FPGA-based system for heart rate calculation based on PPG signal. In: 2017 5th International Conference on Electrical Engineering - Boumerdes, ICEE-B 2017. 2017. https://doi.org/10.1109/ICEE-B.2017.8192157.
13. Johnson MA, Jegan R, Anitha Mary X. Performance measures on blood pressure and heart rate measurement from PPG signal for biomedical applications. In: Proceedings of IEEE International Conference on Innovations in Electrical, Electronics, Instrumentation and Media Technology, ICIEEIMT 2017, 2017. https://doi.org/10.1109/ICIEEIMT.2017.8116856.
14. Das S, Pal S, Mitra M. Real time heart rate detection from PPG signal in noisy environment. In: 2016 International Conference on Intelligent Control, Power and Instrumentation, ICICPI 2016, 2017. https://doi.org/10.1109/ICICPI.2016.7859676.
15. Yang D, Zhu J, Zhu P. SpO2 and heart rate measurement with wearable watch based on PPG. In: IET Conference Publications. 2015. https://doi.org/10.1049/cp.2015.0784.
16. Eklund JM, Khan N. A bio-signal computing platform for real-time online health analytics for manned space missions. IEEE Aerospace Conf Proceed. 2018. https://doi.org/10.1109/AERO.2018.8396819.
17. Khan N, Mikael Eklund J. A highly integrated computing platform for continuous, non-invasive BP estimation. Canadian Conf Electr Comput Eng. 2018. https://doi.org/10.1109/CCECE.2018.8447680.
18. Ghosh S, Banerjee A, Ray N, Wood PW, Boulanger P, Padwal R. Continuous blood pressure prediction from pulse transit time using ECG and PPG signals. In: 2016 IEEE Healthcare Innovation Point-of-Care Technologies Conference, HI-POCT 2016. 2016. https://doi.org/10.1109/HIC.2016.7797728
19. Shriram R, Wakankar A, Daimiwal N, Ramdasi D. Continuous cuffless blood pressure monitoring based on PTT. In: ICBBT 2010 - 2010 International Conference on Bioinformatics and Biomedical Technology. 2010. https://doi.org/10.1109/ICBBT.2010.5479013.
20. Gayathri B, Sruthi K, Menon KAU. Non-invasive blood glucose monitoring using near infrared spectroscopy. In: Proceedings of the 2017 IEEE International Conference on Communication and Signal Processing, ICCSP 2017. 2018. https://doi.org/10.1109/ICCSP.2017.8286555.
21. Paul B, Manuel MP, Alex ZC. Design and development of non invasive glucose measurement system,.In: Proceedings - ISPTS-1, 1st International Symposium on Physics and Technology of Sensors. 2012. https://doi.org/10.1109/ISPTS.2012.6260873.
22. Makovec M, Aljančič U, Vrtačnik D. Evaluation of chronic venous insufficiency with PPG prototype instrument. In: 2017 40th International Convention on Information and Communication Technology, Electronics and Microelectronics, MIPRO 2017 – Proceedings. 2017. https://doi.org/10.23919/MIPRO.2017.7973445.
23. Bhooma G, Kokila S, Jayanthi KK, Kumar VJ. A digital instrument for venous muscle pump test. In: Conference Record - IEEE Instrumentation and Measurement Technology Conference. 2011. https://doi.org/10.1109/IMTC.2011.5944063
24. Khan M, Pretty CG, Amies AC, Elliott RB, Suhaimi FM, Shaw GM, Chase JG. Peripheral venous blood oxygen saturation can be non-invasively estimated using photoplethysmography. In: Proceedings of the Annual International Conference of the IEEE Engineering in Medicine and Biology Society, EMBS. 2015. https://doi.org/10.1109/EMBC.2015.7319858.
25. Clarke GWJ, Chan ADC, Adler A. Effects of motion artifact on the blood oxygen saturation estimate in pulse oximetry. In:

IEEE MeMeA 2014 - IEEE International Symposium on Medical Measurements and Applications, Proceedings. 2014. https://doi.org/10.1109/MeMeA.2014.6860071.
26. Shaltis P, Wood L, Reisner A, Asada H. Novel design for a wearable, rapidly deployable, wireless noninvasive triage sensor. Ann Int Conf IEEE Eng Med Biol - Proceed. 2005. https://doi.org/10.1109/iembs.2005.1617250.
27. Gibbs P, Asada HH. Reducing motion artifact in wearable biosensors using MEMS accelerometers for active noise cancellation. Proceed Am Control Conf. 2005. https://doi.org/10.1109/acc.2005.1470193.
28. Selvi MB, Rajalakshmi S. Extraction and analysis of transabdominal fetal heart rate by NIR Photoplethysmography, Int J Electr Electron Eng. 2015;7. http://www.arresearchpublication.com/images/shortpdf/1427210238_1046.pdf, https://www.semanticscholar.org/paper/EXTRACTION-AND-ANALYSIS-OF-TRANSABDOMINAL-FETAL-BY-Selvi-Rajalakshmi/96730fbd589c3be903ee7aa8baf2bfb18eabc44c.
29. Gan KB, Zahedi E, Ali MAM. Transabdominal fetal heart rate detection using NIR photopleythysmography: instrumentation and clinical results. IEEE Trans Biomed Eng. 2009;56:2075–82. https://doi.org/10.1109/TBME.2009.2021578.
30. Sattar RRM, Chellappan K, Aminuddin A, Omar N, Zakaria Z, Ali MA, Nordin NAMM. Correlation between lipid profile and finger photoplethysmogram morphological properties among young men with cardiovascular risk: a preliminary result. In: IECBES 2014, Conference Proceedings - 2014 IEEE Conference on Biomedical Engineering and Sciences: "Miri, Where Engineering in Medicine and Biology and Humanity Meet". 2014. https://doi.org/10.1109/IECBES.2014.7047574.
31. Zahedi E, Chellappan K, Ali MAM, Singh H. Analysis of the effect of ageing on rising edge characteristics of the photoplethysmogram using a modified windkessel model. Cardiovasc Eng. 2007;7. https://doi.org/10.1007/s10558-007-9037-5.
32. Wang L, Pickwell-MacPherson E, Liang YP, Zhang YT. Noninvasive cardiac output estimation using a novel photoplethysmogram index. In: Proceedings of the 31st Annual International Conference of the IEEE Engineering in Medicine and Biology Society: Engineering the Future of Biomedicine, EMBC 2009. 2009. https://doi.org/10.1109/IEMBS.2009.5333091.
33. Daimiwal N, Sundhararajan M. Non invasive measurement and analysis of cardiac output for different age group using PPG sensor. 2016. https://www.ijcaonline.org/proceedings/ncece2016/number1/24663-9518.
34. Jönsson B, Laurent C, Eneling M, Skau T, Lindberg LG. Automatic ankle pressure measurements using PPG in ankle-brachial pressure index determination. European J Vasc Endovasc Surg. 2005;30. https://doi.org/10.1016/j.ejvs.2005.05.012.
35. Karlen W, Raman S, Ansermino JM, Dumont GA. Multiparameter respiratory rate estimation from the photoplethysmogram. IEEE Trans Biomed Eng. 2013;60. https://doi.org/10.1109/TBME.2013.2246160.
36. Karlen W, Ansermino JM, Dumont G. Adaptive pulse segmentation and artifact detection in photoplethysmography for mobile applications, In: Proceedings of the Annual International Conference of the IEEE Engineering in Medicine and Biology Society, EMBS. 2012. https://doi.org/10.1109/EMBC.2012.6346628.
37. Athaya T, Choi S. An estimation method of continuous noninvasive arterial blood pressure waveform using photoplethysmography: a u-net architecture-based approach. Sensors. 2021;21. https://doi.org/10.3390/s21051867.
38. Chowdhury MH, Shuzan MNI, Chowdhury MEH, Mahbub ZB, Monir Uddin M, Khandakar A, Reaz MBI. Estimating blood pressure from the photoplethysmogram signal and demographic features using machine learning techniques. Sensors (Switzerland). 2020;20. https://doi.org/10.3390/s20113127.
39. Ghosh A, Kalra J. Schr¨odinger spectrum based continuous cuffless blood pressure estimation using clinically relevant features from PPG signal and its second derivative, biomedical signal processing and control. Elsevier. 2023.
40. Samimi H, Dajani HR. A PPG-based calibration-free cuffless blood pressure estimation method using cardiovascular dynamics. Sensors. 2023;23. https://doi.org/10.3390/s23084145.
41. Ibtehaz N, Mahmud S, Chowdhury MEH, Khandakar A, Salman Khan M, Ayari MA, Tahir AM, Rahman MS. PPG2ABP: translating photoplethysmogram (PPG) signals to arterial blood pressure (ABP) waveforms. Bioengineering. 2022;9. https://doi.org/10.3390/bioengineering9110692.
42. Paviglianiti A, Randazzo V, Villata S, Cirrincione G, Pasero E. A comparison of deep learning techniques for arterial blood pressure prediction. Cognit Comput. 2022;14. https://doi.org/10.1007/s12559-021-09910-0.
43. Mehrabadi MA, Aqajari SAH, Zargari AHA, Dutt N, Rahmani AM. Novel blood pressure waveform reconstruction from photoplethysmography using cycle generative adversarial networks. In: Proceedings of the Annual International Conference of the IEEE Engineering in Medicine and Biology Society, EMBS. 2022. https://doi.org/10.1109/EMBC48229.2022.9871962.
44. Samimi H, Dajani HR. Cuffless blood pressure estimation using calibrated cardiovascular dynamics in the photoplethysmogram. Bioengineering. 2022;9. https://doi.org/10.3390/bioengineering9090446.
45. Harfiya LN, Chang CC, Li YH. Continuous blood pressure estimation using exclusively photopletysmography by lstm-based signal-to-signal translation. Sensors. 2021;21. https://doi.org/10.3390/s21092952.
46. Yang S, Sohn J, Lee S, Lee J, Kim HC. Estimation and validation of arterial blood pressure using photoplethysmogram morphology features in conjunction with pulse arrival time in large open databases. IEEE J Biomed Health Inform. 2021;25. https://doi.org/10.1109/JBHI.2020.3009658.
47. Qin K, Huang W, Zhang T. Deep generative model with domain adversarial training for predicting arterial blood pressure waveform from photoplethysmogram signal. Biomed Signal Process Control. 2021;70. https://doi.org/10.1016/j.bspc.2021.102972.
48. Maqsood S, Xu S, Springer M, Mohawesh R. A benchmark study of machine learning for analysis of signal feature extraction techniques for blood pressure estimation using photoplethysmography (PPG). IEEE Access. 2021;9. https://doi.org/10.1109/ACCESS.2021.3117969.
49. Lee D, Kwon H, Son D, Eom H, Park C, Lim Y, Seo C, Park K. Beat-to-beat continuous blood pressure estimation using bidirectional long short-term memory network. Sensors (Switzerland). 2021;21. https://doi.org/10.3390/s21010096.
50. El-Hajj C, Kyriacou PA. Deep learning models for cuffless blood pressure monitoring from PPG signals using attention mechanism. Biomed Signal Process Control. 2021;65. https://doi.org/10.1016/j.bspc.2020.102301.
51. Hsu YC, Li YH, Chang CC, Harfiya LN. Generalized deep neural network model for cuffless blood pressure estimation with photoplethysmogram signal only. Sensors (Switzerland). 2020;20. https://doi.org/10.3390/s20195668.
52. Eom H, Lee D, Han S, Sun Hariyani Y, Lim Y, Sohn I, Park K, Park C. End-to-end deep learning architecture for continuous blood pressure estimation using attention mechanism. Sensors (Switzerland). 2020;20. https://doi.org/10.3390/s20082338.
53. Hasanzadeh N, Ahmadi MM, Mohammadzade H. Blood pressure estimation using photoplethysmogram signal and its

morphological features. IEEE Sens J. 2020;20. https://doi.org/10.1109/JSEN.2019.2961411.
54. Mousavi SS, Firouzmand M, Charmi M, Hemmati M, Moghadam M, Ghorbani Y. Blood pressure estimation from appropriate and inappropriate PPG signals using a whole-based method, Biomed Signal Process Control. 2019;47. https://doi.org/10.1016/j.bspc.2018.08.022.
55. Slapni Č Ar G, Mlakar N, Luštrek M. Blood pressure estimation from photoplethysmogram using a spectro-temporal deep neural network. Sensors (Switzerland). 2019;19. https://doi.org/10.3390/s19153420.
56. Wu D, Xu L, Zhang R, Zhang H, Ren L, Zhang Y-T. Continuous cuff-less blood pressure estimation based on combined information using deep learning approach, J Med Imaging Health Inform. 2018;8. https://doi.org/10.1166/jmihi.2018.2474.
57. Su P, Ding XR, Zhang YT, Liu J, Miao F, Zhao N. Long-term blood pressure prediction with deep recurrent neural networks. In: 2018 IEEE EMBS International Conference on Biomedical and Health Informatics, BHI 2018. 2018. https://doi.org/10.1109/BHI.2018.8333434.
58. Zadi SA, Alex R, Zhang R, Watenpaugh DE, Behbehani K. Arterial blood pressure feature estimation using photoplethysmography. Comput Biol Med. 2018;102. https://doi.org/10.1016/j.compbiomed.2018.09.013.
59. Kachuee M, Kiani MM, Mohammadzade H, Shabany M. Cuffless blood pressure estimation algorithms for continuous health-care monitoring. IEEE Trans Biomed Eng. 2017;64. https://doi.org/10.1109/TBME.2016.2580904.
60. Liu M, Po L-M, Fu H. Cuffless blood pressure estimation based on photoplethysmography signal and its second derivative. Int J Comput Theory Eng. 2017;9:202–6. https://doi.org/10.7763/IJCTE.2017.V9.1138.
61. Zhang Y, Feng Z. A SVM method for continuous blood pressure estimation from a PPG signal. ACM Int Conf Proceed Ser. 2017. https://doi.org/10.1145/3055635.3056634.
62. Xing X, Sun M. Optical blood pressure estimation with photoplethysmography and FFT-based neural networks. Biomed Opt Express. 2016;7. https://doi.org/10.1364/boe.7.003007.
63. Kachuee M, Kiani MM, Mohammadzade H, Shabany M. Cuffless high-accuracy calibration-free blood pressure estimation using pulse transit time. Proceed - IEEE Int Symp Circ Syst. 2015. https://doi.org/10.1109/ISCAS.2015.7168806.
64. Kurylyak Y, Lamonaca F, Grimaldi D. A neural network-based method for continuous blood pressure estimation from a PPG signal. Conf Record - IEEE Instrum Meas Technol Conf. 2013. https://doi.org/10.1109/I2MTC.2013.6555424.
65. Cattivelli FS, Garudadri H. Noninvasive cuffless estimation of blood pressure from pulse arrival time and heart rate with adaptive calibration. In: Proceedings - 2009 6th International Workshop on Wearable and Implantable Body Sensor Networks, BSN 2009. 2009. https://doi.org/10.1109/BSN.2009.35.
66. Saeed M, Villarroel M, Reisner AT, Clifford G, Lehman LW, Moody G, Heldt T, Kyaw TH, Moody B, Mark RG. Multiparameter intelligent monitoring in intensive care II: a public-access intensive care unit database. Crit Care Med. 2011. https://doi.org/10.1097/CCM.0b013e31820a92c6.
67. Johnson AEW, Pollard TJ, Shen L, Lehman LWH, Feng M, Ghassemi M, Moody B, Szolovits P, Anthony Celi L, Mark RG. MIMIC-III, a freely accessible critical care database. Sci Data. 2016;3. https://doi.org/10.1038/sdata.2016.35.
68. Liang Y, Chen Z, Liu G, Elgendi M. A new, short-recorded photoplethysmogram dataset for blood pressure monitoring in China. Sci Data. 2018;5:180020. https://doi.org/10.1038/sdata.2018.20.
69. Khan M, Kumar Singh B, Nirala N. Expert diagnostic system for detection of hypertension and diabetes mellitus using discrete wavelet decomposition of photoplethysmogram signal and machine learning technique. Med Nov Technol Devices. 2023;19:100251. https://doi.org/10.1016/j.medntd.2023.100251.
70. Hu X, Yin S, Zhang X, Menon C, Fang C, Chen Z, Elgendi M, Liang Y. Blood pressure stratification using photoplethysmography and light gradient boosting machine. Front Physiol. 2023;14. https://doi.org/10.3389/fphys.2023.1072273.
71. Islam SMS, Talukder A, Awal MA, Siddiqui MMU, Ahamad MM, Ahammed B, Rawal LB, Alizadehsani R, Abawajy J, Laranjo L, Chow CK, Maddison R. Machine learning approaches for predicting hypertension and its associated factors using population-level data from three South Asian countries. Front Cardiovasc Med. 2022;9. https://doi.org/10.3389/fcvm.2022.839379.
72. Martinez-Ríos E, Montesinos L, Alfaro-Ponce M. A machine learning approach for hypertension detection based on photoplethysmography and clinical data. Comput Biol Med. 2022;145. https://doi.org/10.1016/j.compbiomed.2022.105479.
73. Sun X, Zhou L, Chang S, Liu Z. Using cnn and hht to predict blood pressure level based on photoplethysmography and its derivatives, Biosensors (Basel). 2021;11. https://doi.org/10.3390/bios11040120.
74. Sannino G, De Falco I, De Pietro G. Non-invasive risk stratification of hypertension: a systematic comparison of machine learning algorithms. J Sensor Actuator Networks. 2020;9. https://doi.org/10.3390/JSAN9030034.
75. Liang Y, Chen Z, Ward R, Elgendi M. Hypertension assessment via ECG and PPG signals: an evaluation using MIMIC database. Diagnostics. 2018;8. https://doi.org/10.3390/diagnostics8030065.
76. Liang Y, Chen Z, Ward R, Elgendi M. Photoplethysmography and deep learning: enhancing hypertension risk stratification. Biosensors (Basel). 2018;8. https://doi.org/10.3390/bios8040101.